GSP 4

TASMANIA DEPARTMENT OF MINES

1982

GEOLOGICAL SURVEY
PAPER 4

DISTRIBUTION AND CHARACTERISATION OF GRANITOID INTRUSIONS IN THE BLUE TIER AREA

by M.P. McCLENAGHAN, B.Sc.(Hons), Ph.D.
and P.R. WILLIAMS, B.Sc.(Hons), Ph.D.

DEPARTMENT OF MINES, G.P.O BOX 124B, HOBART, TASMANIA 7001

ISSN 0313 - 1688
ISBN 0 7246 0508 8

McCLENAGHAN, M.P.; WILLIAMS, P.R. 1982. Distribution and characterisation of granitoid intrusions in the Blue Tier area. *Pap.geol.Surv.Tasm.* 4.

ISSN 0313-1688 : ISBN 0 7246 0508 8

CONTENTS

LIST OF FIGURES

LIST OF TABLES

ABSTRACT

The granitoid bodies in the central Blue Tier area are divided into two major categories based on the composition of plagioclase. Alkali-feldspar granite contains dominantly albite and is further subdivided on texture and primary mica composition. Adamellite contains oligoclase-andesine and is also subdivided on textural criteria. There are clear differences in primary mica composition and alteration products between the alkali-feldspar granite and adamellite. The alkali-feldspar granite intrudes the adamellite as a dome-shaped body. The adamellite forms large plutons, domes, and sheets. The alkali-feldspar granite crystallised at a pressure of about 50 MPa and a temperature of about 660°C. The variation in adamellite composition may be due to partial separation of restite material, or fractional crystallisation. The alkali-feldspar granite probably represents residual liquids produced by extreme fractionation, but cannot be derived from the adamellite magma by continued restite separation alone.

INTRODUCTION

The Blue Tier area, 15 km north-west of St Helens in north-east Tasmania (fig. 1) forms the central part of the Blue Tier Batholith. The area contains extensive tin mineralisation and has been studied by Reid and Henderson (1928) and Thomas (1943). The first overall account of the Batholith was that of Groves *et al.* (1977) who subdivided it into eighteen plutons and sheets of distinctive physical characteristics based on reconnaissance geological mapping at a scale of 1:31 680. Recent mapping of the granitoids in the north-western part of the Batholith (at a scale of 1:15 830) by the Geological Survey Branch of the Tasmania Department of Mines also used physical characteristics to delineate rock types, although formal definition of pluton boundaries was not attempted (Brown *et al.*, 1977; Baillie *et al.*, 1978). McClenaghan and Williams (1981; in prep.) have augmented this classification with the composition of plagioclase to define rock units.

The rocks of the Batholith are only weakly deformed, and intruded after the major regional deformation affecting the country rocks. They have narrow contact metamorphic aureoles. All the granitoids are Devonian in age (McDougall and Leggo, 1965), and granodiorites tend to show older radiometric ages than adamellites, which are older than alkali-feldspar granites (Cocker, 1977). However, these age differences are small and often lie within the error range of the stated age.

Geochemical characteristics of the granitoids have been discussed in detail by Groves (1972), Groves and Taylor (1973), Groves *et al.* (1977), Cocker (1977), Groves and McCarthy (1978), McCarthy and Groves (1979), and McClenaghan *et al.* (1982). McCarthy and Groves (1979) argued that the geochemical variations between different plutons can be explained by the progressive accumulation of crystals around the margins of an inwardly crystallizing granitic melt. In this paper, no new evidence regarding the origin of adamellite is put forward, but it is argued that alkali-feldspar granites are highly fractionated rocks and can not be derived from an adamellite source magma by continued unmixing of restite material alone. Cocker (1977) suggested that individual plutons result from crystallisation of melts derived from discrete source rocks of differing chemical compositions.

Widespread late stage alteration of the granitoids has taken place. The alteration is essentially isochemical in all but greisenised rocks. Field relationships in the Blue Tier area suggest that the alkali-feldspar granite forms distinct plutons and that some bodies previously considered to be 'Lottah Sheets' (Groves *et al.*, 1977) and related to tin-bearing granites include adamellite bodies which show geochemical characteristics distinct from the alkali-feldspar granite.

GEOLOGY OF THE BLUE TIER AREA

The granitoid rocks of the Blue Tier area have been subdivided into five adamellite types and two alkali-feldspar granite types (fig. 1). In addition, a number of minor intrusions of silica-rich adamellite, aplite, and a suite of basic to intermediate dykes of probable Devonian age occur in the area (McClenaghan and Williams, 1981).

The major division of the granitoids into two distinct groups (alkali-feldspar granite and adamellite) is based on plagioclase composition. The plagioclase in the alkali-feldspar granite is exclusively albite (An_{0-5}) apart from very rare phenocrysts of oligoclase in the phyric variety, while in the adamellite it is oligoclase or andesine (An_{17-46}). Very thin rims

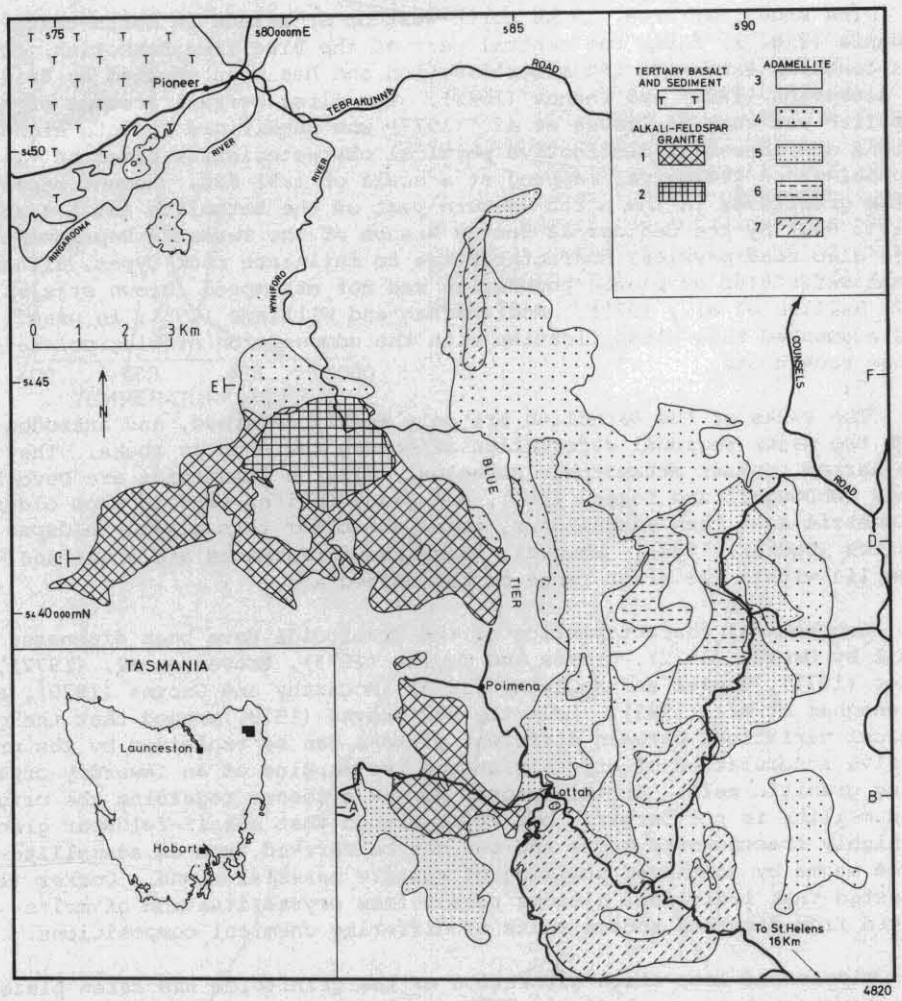

Figure 1. *Geological map of the central Blue Tier area. Rock types indicated by symbols are:*

(1) equigranular alkali-feldspar granite,

(2) phyric alkali-feldspar granite,

(3) phyric coarse-grained adamellite,

(4) phyric medium-grained adamellite,

(5) phyric fine-grained adamellite,

(6) equigranular coarse-grained adamellite, and

(7) hydrothermally altered (greisenised) adamellite.

(<15 μm) of albite occur on the feldspar in the adamellite and are volumetrically insignificant and have not been distinguished separately in modal counts. Feldspar compositions typical of the granitoids are presented in Table 1 and modal analyses in Table 2. The modal data suggests that the quartz content does not vary a great deal between granite types (fig. 3). Further subdivision of the alkali-feldspar granite and adamellite is based on textural features and the type of phenocrysts present. The features which distinguish the various rock types are tabulated in Table 3, which also lists the names used for the bodies in this paper, and the symbol numbers used in Figure 1 and subsequent tables. Previous attempts at subdivision of granitoid types at Blue Tier (Groves *et al.*, 1977; McCarthy and Groves, 1979; Brown *et al.*, 1977; Baillie *et al.*, 1978) relied upon the presence or absence of muscovite as a criterion. This resulted in the inclusion of many adamellite bodies in the same category as alkali-feldspar granite, which is petrologically distinct.

FORM AND MODE OF EMPLACEMENT

The oldest rock type in the map area is the easternmost phyric coarse-grained adamellite (Groves *et al.*, 1977). Boundary relationships between this type and other bodies are not generally well exposed, but several localities contain evidence of the intrusive age relationships and point to an intrusion history. The alkali-feldspar granites were intruded after the major adamellite bodies were emplaced. Evidence of this includes the presence of pegmatitic boundaries of equigranular alkali-feldspar granite against phyric coarse-grained adamellite at Cotton Creek [EQ827433] (McClenaghan *et al.*, 1982), dykes of equigranular alkali-feldspar granite into the adamellite, the presence of greisenised rocks close to roof zones (Groves and Taylor, 1973), and the rectangular form of the alkali-feldspar granite bodies, suggesting dismemberment of the earlier adamellites (*e.g.* at Anchor, EQ848351). The relationship between the coarse-grained equigranular adamellite (rock type 7) and the alkali-feldspar granite is not known.

Figure 2(I) shows the complex form of the adamellite intrusions. The earliest intrusion of phyric coarse-grained adamellite is progressively intruded by the other types. The boundary between the phyric medium-grained adamellite and the phyric coarse-grained adamellite is intrusive on Blue Tier [EQ842439], with coarse pegmatitic patches and greisenisation occurring in the phyric medium-grained adamellite close to the boundary. It is suggested that this is due to the accumulation of volatile phases in the roof zone of the phyric medium-grained adamellite intrusion. Lower down on the eastern side of Blue Tier [EQ907405] the boundary is poorly exposed, but consists of a zone of intimately mixed medium-grained and coarse-grained rocks. At Pioneer [EQ780510] similar phyric medium-grained adamellite is clearly intrusive into the phyric coarse-grained variety.

Fine-grained phyric adamellite on Blue Tier [EQ863386] surrounds a body of medium-grained phyric adamellite. Rafts of the surrounding fine-grained rock, ranging in size up to 10 m in length, are present in the phyric medium-grained rocks. This relationship shows that the fine-grained rocks pre-date the medium-grained rocks, and implies that the medium-grained rocks at the summit ridge of Blue Tier are a dyke-like intrusion close to the dome apex, transecting the pre-existing boundary between the coarse-grained adamellite and the fine-grained body. The fine-grained phyric adamellite forms a sheet in areas where it is not disrupted by the medium-grained adamellite. The sheet dips from 0° to 40° to the west and south-west. The eastern bodies of phyric fine-grained rocks are generally shallow dipping, but have some steeply dipping edges. These edges may be matched, implying

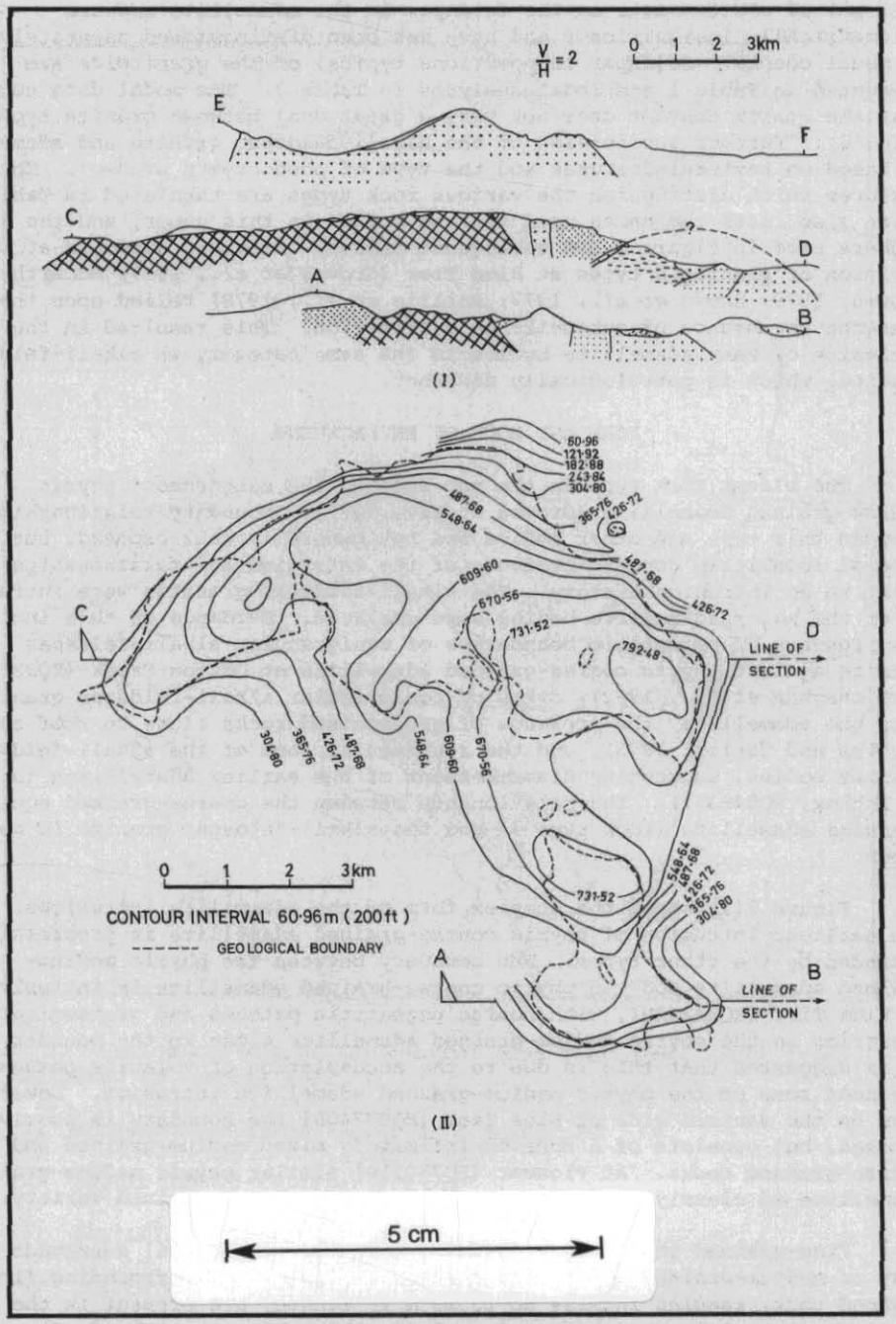

Figure 2. *(I) Diagrammatic E-W geological sections crossing the central Blue Tier area, constructed from topographic information and accurately mapped geological boundaries. See Figure 1 for location of sections and explanation of symbols.*

(II) Structural contours of the boundary of the alkali-feldspar granite with other granitoid bodies. Structural contours determined by combining serial E-W and N-S cross sections, based on mapped boundaries and topographic data.

that they have been pulled apart during intrusion of the medium-grained rocks (*cf.* Gee and Groves, 1971). The thickness changes in the upper fine-grained sheet may be compensated by thickness variations in the lower sheets to which they are probably connected.

Equigranular coarse-grained adamellite intrudes both the fine-grained and medium-grained varieties, as does the greisenised adamellite south of Lottah [EQ856361]. The relationship between the two is not known.

The alkali-feldspar granite, together with the muscovite-bearing adamellite discussed previously, has been ascribed a sheet-like form by Gee and Groves (1971) and Groves and Taylor (1973). It has been argued (McClenaghan *et al.*, 1982) that a sheet-like form is not likely for the alkali-feldspar granite, which is distinguished separately from the muscovite-bearing adamellite bodies, some of which do occur as sheets. The area in the centre of the equigranular alkali-feldspar granite intrusion represents the roof zone of a domal body. The structural contours on the roof of the body are shown in Figure 2(II). Drilling results indicate a depth for the body in excess of 107 m, and show the presence of small sheet-like apophyses of alkali-feldspar granite into the surrounding adamellite (Groves and Taylor, 1973). Gravity results suggest that a considerable body of less dense alkali-feldspar granite exists at depth (Leaman and Symonds, 1975).

PETROGRAPHY OF GRANITOID BODIES

ALKALI-FELDSPAR GRANITE

The alkali-feldspar granite has been divided into a phyric and an equigranular type. The boundaries between phyric and equigranular rocks appear to be gradational over a small distance (McClenaghan *et al.*, 1982).

The equigranular alkali-feldspar granite (fig. 1, rock type 1) is coarse to medium-grained, pink to cream in colour, and composed dominantly of K-feldspar, albite, and quartz (Table 2). Large crystals of albite commonly have sericite alteration of core zones, whereas small crystals are unaltered. Albite also occurs as veinlets which may show incipient polysynthetic twinning. Quartz occurs in two forms: as euhedral crystals with hexagonal cross-section, and as anhedral grain aggregates and veinlets. The grain aggregates and veinlets also contain fairly abundant topaz and annite grains. Perthitic K-feldspar containing abundant euhedral quartz inclusions is euhedral against the quartz aggregates and annite. Non-perthitic or only weakly-perthitic K-feldspar overgrowths on euhedral K-feldspar cores are common. The perthitic K-feldspar is invariably more sodic than the weakly or non-perthitic K-feldspar (Table 1). Accessory minerals are fluorite, zircon, cassiterite and tourmaline, the latter occurring as rare spherical aggregates up to 100 mm in diameter. Muscovite is minor and occurs as an alteration of K-feldspar or derived from the breakdown of annite. Garnet is a rare accessory mineral, sometimes overgrown by biotite, chlorite, and muscovite.

A more leucocratic variety of the equigranular granite occurs in the southern part of the body, and contains zinnwaldite rather than annite as the dominant mica.

The textural features described above suggest two phases of crystallisation for the equigranular granite. The early phase crystallised albite, euhedral quartz, and perthitic K-feldspar with annite intergranular to these minerals. The later phase included the anhedral quartz aggregates

and veinlets, less sodic non or poorly-perthitic K-feldspar, together with annite. Phyric varieties of alkali-feldspar granite (fig. 1, rock type 2) are texturally and mineralogically similar to the equigranular varieties in thin section. The phenocrysts of K-feldspar are string and rod perthite. They are commonly euhedral and are either inclusion free or contain only quartz inclusions. The inclusion free perthite is commonly rimmed by optically continuous non-perthitic K-feldspar which contains abundant annite, plagioclase, and quartz inclusions. The margins of overgrowths are anhedral. Small phenocrysts and aggregates of annite are present. The groundmass of interlocking quartz, non-perthitic K-feldspar, and plagioclase probably formed around early perthite crystals, and some perthite phenocrysts are bent. These features suggest a similar crystallisation sequence to that in the equigranular varieties, with the phenocrysts early-formed and early crystals comprising a lower proportion of the total rock. Quartz phenocrysts are either euhedral crystals or large aggregates of a small number of subhedral quartz grains.

ADAMELLITE

Adamellite is distinguished as having oligoclase or more calcic plagioclase as the dominant plagioclase phase. K-feldspar is abundant as phenocrysts in several types, as well as occurring in the groundmass. The grain size and composition of the phenocrysts serves to subdivide the adamellite into groups.

Phyric coarse-grained adamellite (fig. 1, rock type 3) is the most extensive rock type in the Blue Tier Batholith and belongs to the Poimena Pluton as defined by Groves *et al.* (1977). It is dominantly a biotite adamellite with an average grain size of 5 mm. The modal composition is indicated on Figure 3 and Table 2. K-feldspar perthite is the dominant phenocryst type, and comprises between 10% and 15% of the rock. Phenocrysts may be up to 50 mm long but are usually 25 mm long and commonly aligned. They contain abundant zones of plagioclase inclusions aligned parallel to crystal faces. Crystals contain up to five such zones. The K-feldspar perthite has anhedral boundaries with the surrounding minerals. Muscovite, biotite, and quartz inclusions are also present in phenocrysts of K-feldspar. Muscovite flakes always occur within or adjacent to K-feldspar. Biotite is abundant and occurs as euhedral flakes, some of which are altered to chlorite and others to chlorite and epidote. Iron oxide grains are abundant and occur as vein fillings and along grain boundaries. They appear to be secondary, possibly related to the biotite breakdown. Apatite is a minor phase.

Phyric medium-grained adamellite (fig. 1, rock type 4) has an average groundmass grain size between 1 mm and 5 mm. Plagioclase phenocrysts are abundant and range in length up to 5 mm. K-feldspar phenocrysts are also common and are usually about 20 mm long. Rounded phenocrysts of quartz are up to 5 mm in diameter. Modal analysis of the rock's major components is shown in Figure 3 and Table 2. K-feldspar phenocrysts are string perthites with incipient microcline cross-hatched twinning. They contain abundant inclusions of biotite, euhedral muscovite, quartz, and sericitised plagioclase aligned parallel to the crystal faces. The biotite inclusions are fresh, rust-brown in colour, and have abundant zircon inclusions. The plagioclase inclusions show sericitic alteration. They are also strongly zoned with an albite rim, probably resulting from reaction with the enclosing K-feldspar. The phenocrysts are euhedral against groundmass K-feldspar and are therefore probably earlier than the groundmass crystals. Rare phenocrysts are surrounded by rims of plagioclase. The groundmass

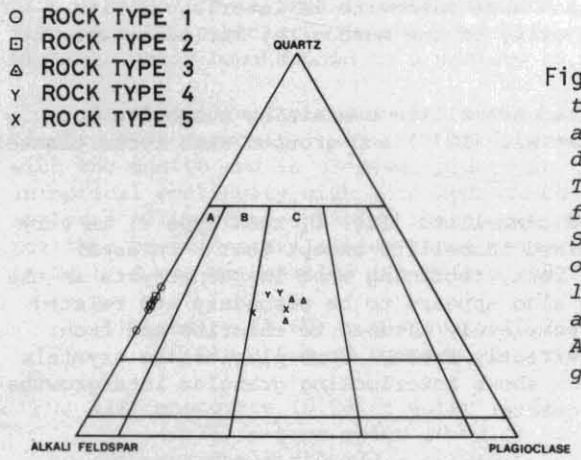

Figure 3. *Modal analyses of granitoids from the central Blue Tier area. Rock type numbers are defined in Figure 1 and Table 3. The classification used is modified from that recommended by the IUGS Subcommission on the Systematics of Igneous Rocks (Streckeisen, 1973) to include granite (field B) and adamellite (field C). Field A represents alkali-feldspar granite.*

K-feldspar contains sericitic-kaolinitic cores with unaltered rims about 0.1 mm wide. Other groundmass-sized K-feldspar is fresh and perthitic. Some myrmekitic grains occur as small patches and on grain boundaries. Plagioclase phenocrysts are commonly zoned and contain altered zones within them. They usually have a rim of probably albitic composition. Some large, strongly sericitised plagioclase grains are also present. The composition of the phenocryst plagioclase is An_{30}, based on measurements of extinction angles.

The dominant mica in this rock type is subhedral, reddish-brown biotite with zircon inclusions. In places the biotite is interleaved with chlorite, and in these grains there are associated opaque (iron oxide) grains. There are also intergrowths of muscovite with the chlorite and biotite. This rock type also contains abundant apatite grains. A small percentage of muscovite flakes are euhedral and fresh and apparently not related to biotite or K-feldspar.

Phyric fine-grained adamellite (fig. 1, rock type 5) occurs as discrete sheet-like bodies intruded at various levels in the batholith. The rock is light grey in colour and contains sparse K-feldspar phenocrysts (20 mm long) and abundant plagioclase phenocrysts (10 mm long) in a fine-grained groundmass of quartz, K-feldspar, and plagioclase of average size less than 1 mm. Quartz phenocrysts are also abundant (up to 5 mm). Modal analyses of the major components are shown in Figure 3 and Table 2. The rock characteristically contains small amounts of apatite and topaz (<1%) as well as biotite, muscovite, chlorite, and opaque mineral grains (iron oxide). Plagioclase phenocrysts sometimes have narrow rims composed of myrmekitic intergrowths. They contain very few inclusions, notably quartz and rarely biotite and chlorite. They are subhedral, due to the partial reaction of the phenocryst with the surroundings, evidenced by resorbed crystals and scalloped boundaries. Plagioclase phenocrysts are rarely sericitised. Quartz phenocrysts are subhedral, and in most specimens contain only rare biotite inclusions. K-feldspar phenocrysts contain inclusions of phengitic muscovite, biotite, plagioclase, and quartz. They tend to be subhedral.

The dominant mica in most specimens is dark reddish-brown biotite which is characteristically altered to green chlorite and iron oxide. Muscovite is present ubiquitously, and in some rock exceeds biotite in abundance. In such cases large flakes poikilitically enclose a large number of matrix grains and are clearly late minerals. Muscovite also occurs as an alteration product of K-feldspar. Well crystallised muscovite grains often

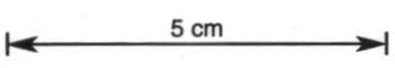

transect altered biotite flakes and some muscovite is interleaved with chlorite, suggesting that the majority of the muscovite, including the homogeneous flakes, is secondary.

Bodies of phyric fine-grained adamellite containing muscovite were classed as 'granites' by Groves *et al.* (1977) and grouped with rocks classed here as alkali-feldspar granite.

Equigranular coarse-grained adamellite (fig. 1, rock type 6) is very similar to the phyric coarse-grained adamellite except that K-feldspar perthite is more abundant in the rock, replacing that in phenocrysts in the phyric variety. Minor muscovite also appears to be secondary and related to K-feldspar. Some biotite is completely altered to chlorite and iron oxide, whereas some grains are perfectly fresh. Some plagioclase crystals show oscillatory zoning. The rock shows interlocking granular intergrowths of plagioclase, orthoclase, and quartz.

In the adamellite bodies, the dominant textural features of interlocking granular to hypidiomorphic granular aggregates of groundmass quartz, plagioclase, and K-feldspar suggest contemporaneous crystallisation. In phyric varieties, the K-feldspar phenocrysts have euhedral to subhedral boundaries, and zones of crystallographically aligned small inclusions. This implies that the phenocrysts attained their present size prior to the crystallisation of the bulk of the groundmass. Plagioclase and quartz show resorbed boundaries and sometimes secondary rims. K-feldspar crystals with plagioclase rims may be xenocrystic. In summary, the major differences between the adamellite types are the virtual absence of muscovite in the phyric coarse-grained rocks (Table 2) and the grain size and texture of the fine and medium-grained varieties.

The body of altered granite (fig. 1, rock type 7) to the south-east of the main alkali-feldspar granite mass is a fine-grained light grey rock which is generally equigranular with variably developed sparse small plagioclase and quartz phenocrysts. The groundmass consists of perthitic K-feldspar, quartz, plagioclase, muscovite, and biotite. Plagioclase in the rock is variable in composition (An_{0-13}, Table 1). Biotite is frequently largely altered to muscovite and sometimes to chlorite. Muscovite is also present as an alteration product of K-feldspar and as large irregular flakes associated with minor amounts of topaz. The amount of feldspar and muscovite is highly variable, and in some cases the rock is composed almost entirely of quartz and muscovite.

PETROLOGY OF GRANITOID BODIES

COMPARATIVE MINERALOGY

Alkali-feldspar granite and adamellite show distinctive mineralogical differences, particularly in their sheet silicate and plagioclase components. Proposed reactions for the sub-solidus decomposition of the primary sheet silicates also differ. Table 1 shows characteristic feldspar compositions of both granitoid types. Plagioclase zonation and K-feldspar compositions do not vary greatly between adamellite bodies, and the examples selected in Table 1 are typical of most adamellite types (3, 4, 5, and 6). Albite composition is consistent throughout the alkali-feldspar granite bodies, but two groups of K-feldspar compositions are present, differing in the proportion of the albite component in solid solution. Table 4 shows the analyses of typical sheet silicates and some of the accessory minerals present in the different rock types. Alkali-feldspar granites are characterised by having annite or zinnwaldite as the primary mica composi-

tion. Muscovite is usually secondary and is more iron-rich than muscovite from adamellite bodies. In the adamellite bodies the dominant mica is biotite, which breaks down to a variety of secondary minerals.

In alkali-feldspar granite, annite is in physical and optical continuity with muscovite, and iron oxide grains are usually present in contact with the annite and in cleavage planes in the muscovite. Muscovite is also in optical continuity with both hydromuscovite(?) and kaolinite. Microprobe analyses of these co-existing phases are presented in Tables 4-6. Three possible reactions explaining these textures and using the chemical analyses in Table 4 can be modelled (Le Maitre, 1979) by simple decomposition:

(1) annite (1.00) → muscovite (0.76) + iron oxide (0.23) + water (0.01). Sum of squares of residuals = 2.691.

(2) muscovite (0.95) + water (0.05) → kaolinite (0.61) + K-feldspar (0.31) + iron oxide (0.03) + KOH (0.05). Sum of squares of residuals = 0.237.

(3) muscovite (0.99) + water (0.01) → hydromuscovite(?) (0.90) + iron oxide (0.02) + KOH (0.08). Sum of squares of residuals = 1.348.

The values in brackets are the proportions of the mineral involved in the calculation.

The adamellite alteration assemblages are characterised by ubiquitous chlorite and iron oxide grains in intimate association with biotite. This is in marked contrast with the alkali-feldspar granite, which is virtually devoid of chlorite. The presence of secondary sphene and epidote-like minerals appears characteristic of the coarse and medium-grained phyric adamellite, whereas muscovite and hydromica are the common secondary mica in the fine-grained phyric adamellite. Microprobe analyses of biotite and coexisting secondary minerals in the adamellite bodies are shown in Tables 4-6. Possible reactions involving these phases and analysed feldspar (Table 7) are modelled below for the medium and coarse-grained phyric adamellite:

(4) biotite (0.74) + plagioclase (0.23) + water (0.03) → chlorite (0.56) + epidote (0.06) + K-feldspar (0.34) + ilmenite (0.04). Sum of squares of residuals = 1.110.

(5) biotite (0.67) + plagioclase (0.30) + water (0.03) → chlorite (0.50) + K-feldspar (0.41) + sphene (0.09). Sum of squares of residuals = 4.502.

(6) biotite (0.98) + water (0.02) → chlorite (0.48) + muscovite (0.33) + K-feldspar (0.19). Sum of squares of residuals = 7.097.

In the phyric fine-grained adamellite, biotite may break down by reaction (7):

(7) biotite (0.96) + water (0.04) → chlorite (0.05) + muscovite (0.58) + ilmenite (0.05) + K-feldspar (0.29) + KOH (0.03). Sum of squares of residuals = 5.351.

The release of KOH is implied when muscovite compositions have a lower K_2O value than ideal. In these rocks, illite and kaolinite are produced by the breakdown of muscovite, in reactions similar to those

Table 1. COMPOSITIONS OF CHARACTERISTIC PLAGIOCLASE AND K-FELDSPAR FROM GRANITOIDS IN THE BLUE TIER AREA

Rock Type'	1,2	1,2	1,2	3	3	3	3	7	7
Mineral	Perthite	K-feldspar	Albite	Zoned Plagioclase			Perthite	Plagioclase	
				Core	Centre	Rim			
SiO_2	65.54	65.04	68.42	57.82	60.97	65.76	65.63	65.04	68.50
Al_2O_3	17.89	17.93	20.17	26.66	24.70	21.79	17.89	21.91	19.71
CaO	1.42	0.99	0.78	9.29	6.91	3.34	1.39	2.70	0.40
Na_2O	2.99	0.21	10.06	5.99	7.01	8.84	1.86	9.67	10.59
K_2O	12.01	15.83	0.56	0.25	0.42	0.27	13.25	0.43	0.80
Structural Formulae (based on 32 oxygens)									
Si	11.983	12.020	11.935	10.355	10.835	11.538	12.027	11.453	11.976
Al	3.875	3.906	4.147	5.627	5.173	4.505	3.865	4.547	4.060
Na	1.062	0.076	3.405	2.078	2.415	3.008	0.660	3.303	3.592
Ca	0.289	0.197	0.145	1.782	1.316	0.628	0.271	0.509	0.076
K	2.802	3.733	0.126	0.057	0.095	0.059	3.097	0.097	0.176
Σ	20.011	19.931	19.757	19.902	19.836	19.741	19.923	19.973	19.880
Molecular Proportions (%)									
An	6.96	4.92	3.94	45.99	34.39	17.01	6.75	13.02	1.98
Ab	25.57	1.90	92.63	53.03	63.11	81.39	16.40	84.50	93.44
Or	67.47	93.18	3.43	1.47	2.50	1.60	76.85	2.48	4.58
Nϕ	5	13	16	2	2	2	19	3	4

' Rock Type Numbers 1. Equigranular alkali-feldspar granite, 2. Phyric alkali-feldspar granite, 3. Phyric coarse-grained adamellite, 7. Greisenised adamellite, Anchor area.

ϕ N is the number of analyses from which the analysis is chosen.

Table 2. MODAL COMPOSITION OF TYPICAL SPECIMENS OF GRANITOIDS, CENTRAL BLUE TIER AREA

Specimen	Rock typeϕ	K-feldspar	Plagioclase	Quartz	Biotite (*Annite)	Muscovite (*Zinnwaldite)	Nos. of counts	Grid size (mm)	Grain-size (mm)
802640	1	43.45	23.92	25.68	0	6.86*	1998	5	2
742518	1	32.82	23.75	35.94	6.20*	1.24	1764	5	3
742528	1	37.98	24.84	30.95	5.54*	0.70	1522	5	3
73-694†	1	31.53	30.00	32.23	3.80*	0.80	3000	0.33	0.4
J74-8	1	33.16	29.70	34.64	1.08*	1.34	5000	0.33	0.4
802647	2	39.36	21.56	34.92	3.12*	1.04	1498	5	2
J74-16	2	38.1	23.9	31.8	5.4*	0.6	5000	0.33	0.4
BT3-41	3	29.06	32.04	33.22	5.67	0	2993	5	5
735702	3	35.52	30.69	28.20	5.60	0	1360	5	2.5
735703	3	32.86	30.86	34.96	1.32	0	3686	5	3
802646	4	33.54	22.17	32.49	8.7	3.1	1619	5	3
BT3-45	4	34.26	27.06	36.47	1.46	0.75	1722	2	5
802628	5	41.38	22.85	30.58	3.46	1.73	3816	2	0.7
802619	5	33.80	29.48	31.29	3.26	2.17	2154	2	0.7

† includes 1.6% topaz

ϕ see Table 3 for explanation of rock types

Table 3. PETROGRAPHIC AND PHYSICAL FEATURES USED TO DISTINGUISH GRANITOIDS, CENTRAL BLUE TIER AREA

Plagioclase composition	Texture	Phenocryst composition	Mica composition	Grain size	Symbol number	Rock name
Albite	Equigranular	-	Biotite + muscovite	Medium	1	Equigranular alkali-feldspar granite
Albite	Phyric	Quartz + K-feldspar	Biotite	Medium	2	Phyric alkali-feldspar granite
Oligoclase-andesine	Phyric	Orthoclase	Biotite	Coarse	3	Phyric coarse-grained adamellite
Oligoclase-andesine	Phyric	Plagioclase + orthoclase + quartz	Biotite + muscovite	Medium	4	Phyric medium-grained adamellite
Oligoclase-andesine	Phyric	Plagioclase + quartz + orthoclase	Biotite + muscovite	Fine	5	Phyric fine-grained adamellite
Oligoclase-andesine	Equigranular	-	Biotite	Coarse	6	Equigranular coarse-grained adamellite
Albite-oligoclase	Phyric-equigranular	Quartz + orthoclase	Muscovite + biotite	Fine	7	Altered (greisenised) adamellite

Table 4. SHEET SILICATE AND ACCESSORY MINERAL ANALYSES FROM BLUE TIER GRANITOIDS

Rock Type'	1	1	1	1	1	1	2	2	3
Mineral	Annite	Zinn-waldite	Muscovite	Hydro-Muscovite(?)	Kaolinite	Garnet	Annite	Muscovite	Biotite
SiO_2	34.73	44.32	47.05	51.23	47.09	35.07	35.15	46.41	34.37
TiO_2	0	0.28	0	0	0	0.29	0.87	0	4.32
Al_2O_3	22.52	21.98	30.12	34.32	37.74	20.19	21.46	31.30	14.54
FeO	27.40	17.94	6.45	4.45	0.76	25.14	27.00	5.66	24.92
MnO	0.89	0.39	0	0	0	16.80	0.73	0	0.67
MgO	0.32	0	0	0	0	0.55	0.60	0	7.43
CaO	0.59	0.69	0.69	0.30	0	1.71	0.70	0.77	0.72
Na_2O	0.37	0	0	0	0	0	0	0	0
K_2O	9.37	10.30	11.31	4.88	0.54	0	9.66	11.47	9.22
H_2O+	3.83	4.10	4.38	4.61	13.86	0	3.83	4.39	3.82
Structural Formulae (number of oxygen atoms per formula unit indicated)									
	22	22	22	22	14	24	22	22	22
Si	5.442	6.475	6.441	6.612	4.072	5.825	5.501	6.339	5.398
Al	2.558	1.525	1.559	1.338	0	0.175	2.499	1.661	2.602
Σ	8.000	8.000	8.000	8.000	4.072	6.000	8.000	8.000	8.000
Al	1.602	2.262	3.302	3.822	3.847	3.777	1.460	3.380	0.089
Ti	0	0.030	0	0	0	0.036	0.103	0	0.509
Fe^{+2}*	3.591	2.193	0.738	0.480	0.055	3.493	3.535	0.647	3.273
Mn	0.118	0.049	0	0	0	2.364	0.096	0	0.089
Mg	0.075	0	0	0	0	0.136	0.141	0	1.739
Σ	5.386	4.534	4.040	4.328	3.902	-	5.335	4.027	5.699
Ca	0.099	0.108	0.101	0.041	0	0.304	0.117	0.113	0.121
Na	0.115	0	0	0	0	0	0	0	0
K	1.872	1.918	1.975	0.802	0.060	0	1.930	1.998	1.848
Σ	2.086	2.026	2.109	0.843	0.060	10.144	2.047	2.111	1.970
OH†	4.000	4.000	4.000	4.000	8.000	0	4.000	4.000	4.000
Nϕ	2	5	5	1	1	1	4	2	5

' Rock Type Numbers 1. Equigranular alkali-feldspar granite, 2. Phyric alkali-feldspar granite, 3. Phyric coarse-grained adamellite, 4. Phyric medium-grained adamellite, 5. Phyric fine-grained adamellite, 7. Greisenised adamellite

* All Fe calculated as FeO, † H_2O and OH calculated as for ideal formulae, ϕ N is the number of analyses from which the analysis is chosen.

Table 5. SHEET SILICATE AND ACCESSORY MINERAL ANALYSES FROM BLUE TIER GRANITOIDS

Rock Type'	3	3	3,4	3	4	4	4	4	5
Mineral	Muscovite	Chlorite	Epidote	Sphene	Biotite	Muscovite	Altered biotite	Chlorite	Biotite
SiO_2	47.75	24.80	37.48	32.41	34.31	46.72	40.55	26.12	34.34
TiO_2	0.21	0.20	3.30	30.21	3.47	0.43	0.47	0.75	3.24
Al_2O_3	32.23	20.01	20.92	6.65	18.42	34.95	24.12	17.95	19.45
FeO	2.56	31.01	14.58	2.15	22.10	1.45	17.11	31.79	22.52
MnO	0	0.79	0.21	0	0.36	0	0.32	0.63	0.41
MgO	1.16	11.13	4.08	0	6.99	0	6.24	10.42	5.82
CaO	0.72	0	16.88	28.57	0.62	0.64	0.62	0.42	0.64
Na_2O	0.82	0.41	0	0	0.38	0	0.69	0	0.22
K_2O	10.06	0.24	0.42	0	9.47	11.31	5.72	0.52	9.47
H_2O+	4.49	11.09	1.85	0	3.89	4.50	4.17	11.04	3.89
Structural Formulae (number of oxygen atoms per formula unit indicated)									
	22	28	25	20	22	22	22	28	22
Si	6.380	5.367	6.083	4.196	5.291	6.229	5.819	5.670	5.293
Al	1.620	2.633	–		2.709	1.771	2.181	2.330	2.707
Σ	8.000	8.000	6.083	4.196	8.000	8.000	8.000	8.000	8.000
Al	3.456	2.469	4.000	1.015	0.637	3.722	1.898	2.264	0.826
Ti	0.021	0.034	0.403	2.941	0.403	0.043	0.051	0.123	0.376
Fe^{+2}*	0.285	5.610	1.978	0.232	2.851	0.163	2.054	5.772	2.903
Mn	0	0.143	0.029	0	0.047	0	0.038	0.116	0.055
Mg	0.231	3.588	0.987	0	1.605	0	1.335	3.371	1.336
Σ	3.993	–	–	4.188	5.543	3.928	5.376	–	5.496
Ca	0.103	0	2.936	3.964	0.103	0.091	0.095	0.097	0.106
Na	0.204	0.169	0	0	0.113	0	0.193	0	0.066
K	1.714	0.067	0.088	0	1.862	1.923	1.046	0.144	1.862
Σ	2.031	12.138	10.457	3.964	2.078	2.014	1.334	11.951	2.034
OH†	4.000	16.000	2.000	0	4.000	4.000	4.000	16.000	4.000
Nϕ	1	11	3	1	3	3	1	5	3

', *, †, ϕ See Table 4 for explanation.

Table 6. SHEET SILICATE AND ACCESSORY MINERAL ANALYSES FROM BLUE TIER GRANITOIDS

Rock Type'	5	5	5	5	7	7	7	7	7
Mineral	Muscovite	Altered biotite	Chlorite	Ilmenite	Biotite	Muscovite	Altered biotite	Kaolinite	Chlorite
SiO_2	46.39	35.40	25.90	0	34.14	46.60	41.89	45.77	25.59
TiO_2	0.44	3.56	0.24	51.25	2.93	0.23	0.50	0.38	0.21
Al_2O_3	34.94	19.03	18.55	0.67	19.69	34.60	29.05	36.70	23.20
FeO	1.45	24.51	33.28	42.07	23.40	1.94	15.23	2.38	28.68
MnO	0	0.43	0.57	4.51	0.28	0	0.33	0	0.57
MgO	0	6.25	10.00	0.66	5.55	0.26	3.19	0.34	9.62
CaO	0.78	2.92	0	0	0.60	0.66	0.67	0.21	0
Na_2O	0	0	0	0.84	0	0	0	0	0.86
K_2O	11.52	3.94	0.20	0	9.53	11.23	4.41	0.52	0.28
H_2O+	4.49	3.97	11.01	0	3.89	4.48	4.50	13.70	11.28
Structural Formulae (number of oxygen atoms per formula unit indicated)									
	22	22	28	6	22	22	22	14	28
Si	6.200	5.348	5.369	0	5.278	6.229	5.582	4.003	5.487
Al	1.800	2.652	2.361	0	2.722	1.771	2.418	0	2.513
Σ	8.000	8.000	8.000	0	8.000	8.000	8.000	4.003	8.000
Al	3.704	0.737	2.399	0.040	0.867	3.680	2.365	3.785	3.098
Ti	0.045	0.404	0.040	1.942	0.340	0.023	0.052	0.025	0.033
Fe^{+2}*	0.161	3.097	6.059	1.773	3.025	0.217	1.779	0.174	5.098
Mn	0	0.054	0.105	0.192	0.036	0	0.039	0	0.103
Mg	0	1.408	3.244	0.050	1.279	0.051	0.666	0.044	3.074
Σ	3.910	5.700	-	-	5.547	3.971	4.928	4.028	-
Ca	0.112	0.473	0	0	0.100	0.094	0.100	0.019	0
Na	0	0	0	0.082	0	0	0	0	0.360
K	1.964	0.761	0.055	0	1.880	1.915	0.786	0.058	0.077
Σ	2.076	1.234	11.947	4.097	1.980	2.009	0.886	0.077	11.877
OH†	4.000	4.000	16.000	0	4.000	4.000	4.000	8.000	16.000
Nϕ	5	2	4	1	2	2	2	2	2

', *, †, ϕ See Table 4 for explanation.

Table 7. CHEMICAL ANALYSES FROM GRANITOIDS, BLUE TIER AREA, SHOWING THE COMPOSITIONAL RANGE OF THE MAJOR TYPES

Rock type number*	1	1	2	2	3	3	4	5	5
Analysis number	742516	742608	742520	742528	742515	735711	742533	735712	742607
SiO_2	76.10	73.50	75.80	76.00	74.00	70.40	72.40	72.00	75.40
TiO_2	0.01	0.03	0.05	0.02	0.25	0.42	0.29	0.29	0.10
Al_2O_3	13.90	15.10	13.20	13.50	14.20	13.80	14.30	13.90	13.70
Fe_2O_3	0.05	0.37	0.42	0.29	0.42	0.83	0.55	0.57	0.53
FeO	1.20	0.52	0.75	1.40	1.40	2.40	1.60	1.70	0.52
MnO	0.05	0.04	0.04	0.04	0.05	0.06	0.05	0.04	0.04
MgO	0.02	0.01	0.07	0.03	0.55	0.75	0.64	0.50	0.16
CaO	0.37	0.43	0.40	0.45	1.60	2.10	1.60	1.20	0.53
Na_2O	3.60	4.20	3.10	3.30	3.10	3.00	3.00	2.70	3.30
K_2O	4.50	3.90	4.80	4.70	4.60	3.90	4.70	5.10	4.80
P_2O_5	0.09	0.36	0.06	0.08	0.10	0.15	0.14	0.15	0.12
H_2O^+	0.74	0.35	0.57	0.65	0.80	1.40	0.97	1.30	0.42
H_2O^-	0	0	0	0	0	0	0	0	0.14
CO_2	0.13	0.07	0.04	0.34	0.12	0	0.02	0	0.08
Total	100.76	98.88	99.30	100.80	101.19	99.21	100.26	99.45	99.84
Li	260	465	148	130	84	90	70	65	15
F	4900	3900	2800	4200	1000	nd	600	nd	500
Rb	848	1650	635	599	287	350	277	460	311
Sr	6	15	14	8	105	135	121	95	45
Y	46	6	43	40	38	50	34	40	32
Zr	33	19	65	36	117	185	137	155	49
Nb	22	76	17	16	17	nd	20	nd	11
Sn	29	42	27	25	15	24	12	25	22

* For an explanation of rock type numbers, see Table 4.
nd = not determined
Analyst: J. Furst, Department of Mines, Launceston
A complete list of analyses is available on request

indicated for the alkali-feldspar granite. The reactions involved in the greisenised adamellite do not yield good fits on the reactions modelled, and are inferred to be non-isochemical. The composition of white-mica and biotite from these greisenised rocks is similar to the composition in the other adamellite bodies (Table 6), and together with the presence of chlorite and oligoclase, suggests that this rock type is derived from an adamellite host, rather than an alkali-feldspar granite.

GEOCHEMISTRY

Major and trace element analyses of adamellite and alkali-feldspar granite covering the range of composition of the various granitoid types are given in Table 7. Harker variation diagrams for all the analysed rocks are presented in Figure 4. On these diagrams, poorly defined linear trends are apparent for the coarse-grained phyric adamellite (rock type 3) and the fine-grained phyric adamellite (rock type 5) for TiO_2, CaO, and Rb, while for MgO and Sr, the trends are less clear. Slight differences between the trends for the two rock types can be seen, particularly in the case of CaO. Two analyses of the phyric medium-grained adamellite (rock type 4) plot with the coarse-grained phyric adamellite.

The alkali-feldspar granites define trends for the oxides and trace elements plotted with the porphyritic granite (rock type 2) lying at the high SiO_2 end of the trends. The equigranular granite, which plots separately at a lower SiO_2 value than the others but on the same trend, is the leucocratic variant. It seems probable that rocks of intermediate composition between this sample and the normal equigranular granite exist, as the two rock types grade into each other. The plot of Rb against SiO_2 shows that there is a clear difference between the equigranular and the porphyritic alkali-feldspar granite, which is also evident in the K_2O and Na_2O values (Table 5).

The alkali-feldspar granites overlap with the adamellites in SiO_2 value but there is a clear compositional gap for most other elements. This gap is particularly clear on a Ti/10-Rb/3-Sr diagram (fig. 5).

The straight line trends in the adamellite compositions shown in the variation diagrams (fig. 4) may be explained by either of two genetic models. The first of these is the restite model (White and Chappell, 1977). However there is no conclusive textural evidence that the adamellite contains any restite material. Sericite-rich plagioclase overgrown by unaltered plagioclase is the only material that might be suggested as being restite. The plagioclase grains are strongly zoned (Table 1). The second model is fractional crystallisation, or a variation on this such as cumulate fractional crystallisation (McCarthy and Groves, 1979). Textural evidence was also lacking to support the cumulate fractional crystallisation model.

The close spatial and temporal relationship between the adamellite and the alkali-feldspar granite suggests that they may be genetically related. The alkali-feldspar granite compositions could not be produced by continued unmixing of restite material from the same magma from which the adamellite was derived because they depart considerably from the adamellite trends on the variation diagrams for most elements (fig. 4). This conclusion is in agreement with that reached by McCarthy and Groves (1979). In addition, the extremely low K/Rb ratios (generally in the range 40-70) of the alkali-feldspar granite suggest that they are the product of extreme fractionation (Taylor, 1965).

Among the alkali-feldspar granites, the porphyritic granite lies

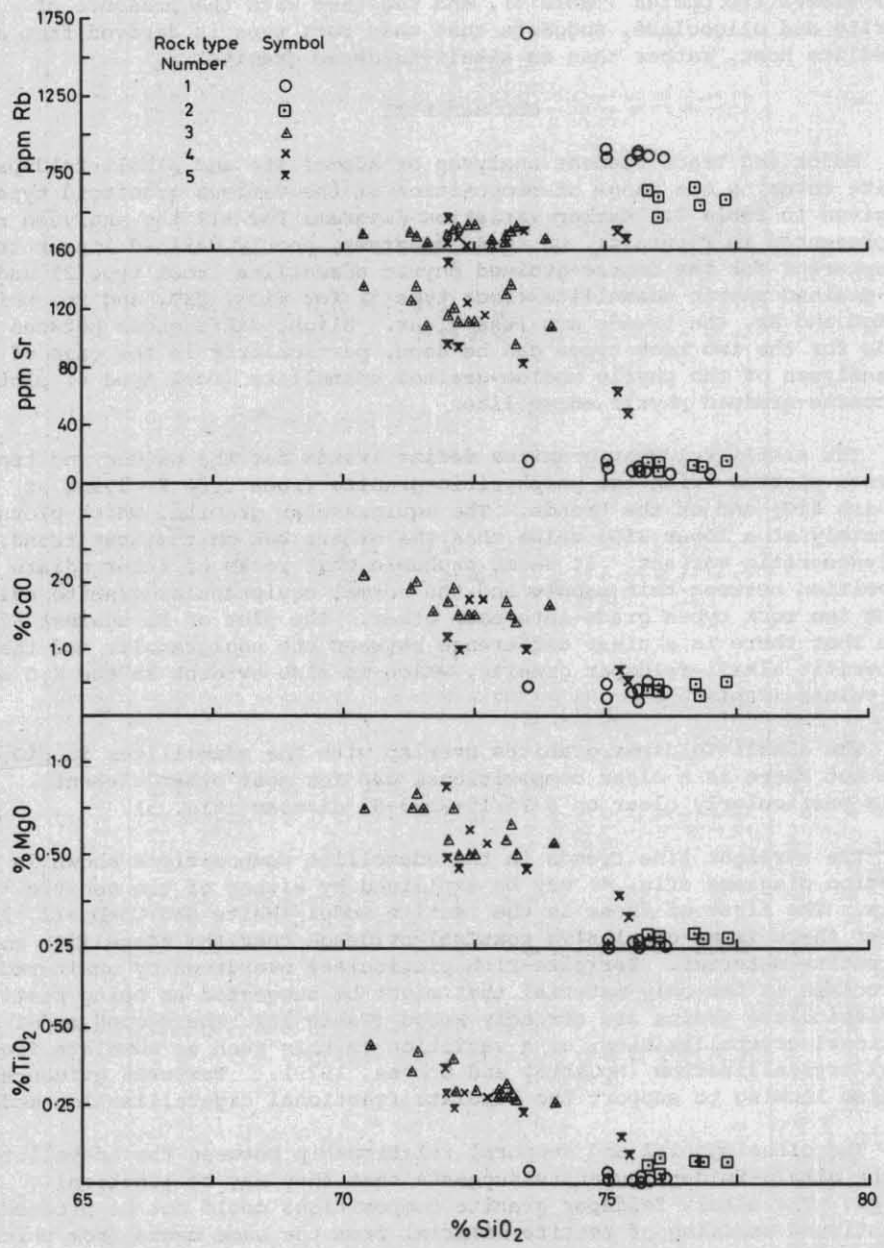

Figure 4. *Harker diagrams for various oxides and elements of the central Blue Tier granitoids.*

5 cm

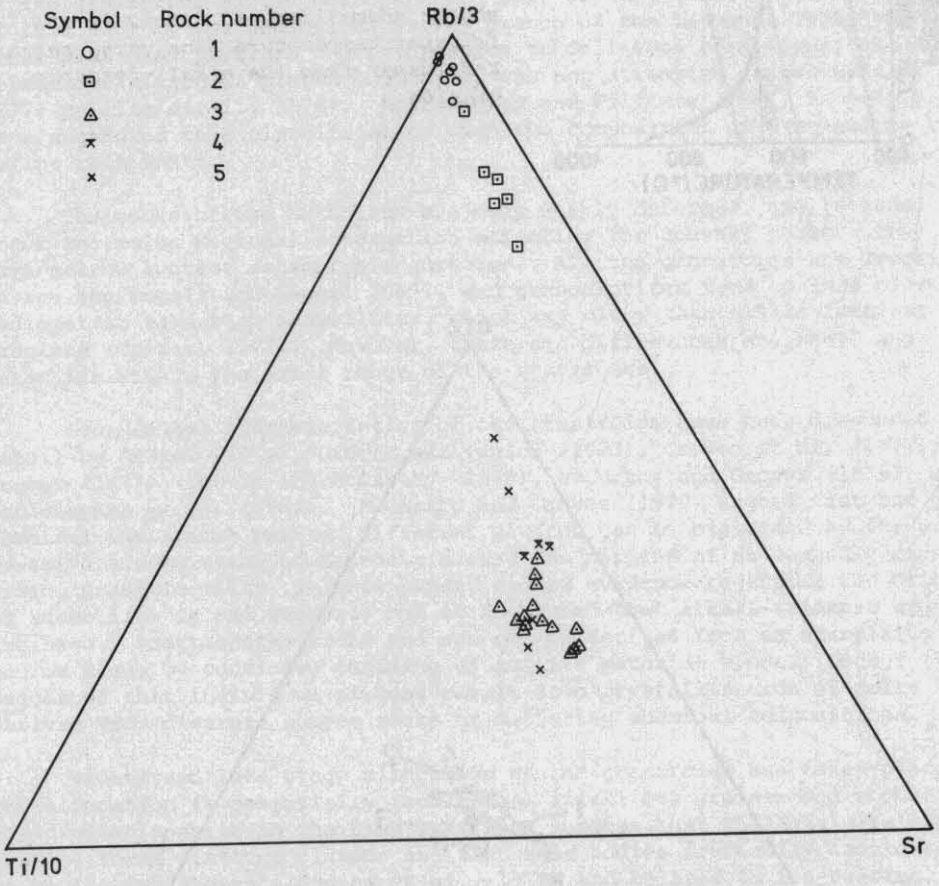

Figure 5. *Triangular discrimination diagram for central Blue Tier granitoids.*

(1) equigranular alkali-feldspar granite,

(2) phyric alkali-feldspar granite,

(3) phyric coarse-grained adamellite,

(4) phyric medium-grained adamellite,

(5) phyric fine-grained adamellite.

5 cm

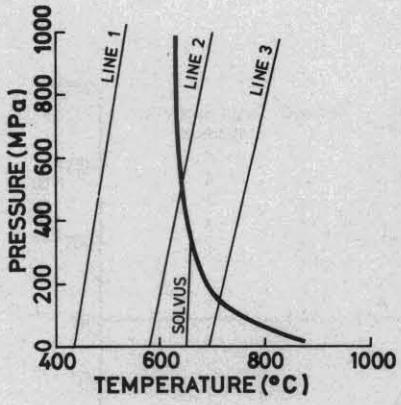

Figure 6. *Pressure-temperature diagram for the granite solidus (Luth et al., 1964), the alkali-feldspar solvus (Yoder et al., 1957; Orville, 1963), and feldspar temperature lines. Lines 1 and 3 are the lowest and highest feldspar temperature lines for the coarse-grained phyric adamellite and line 2 is the feldspar temperature line using perthitic K-feldspar from the alkali-feldspar granite.*

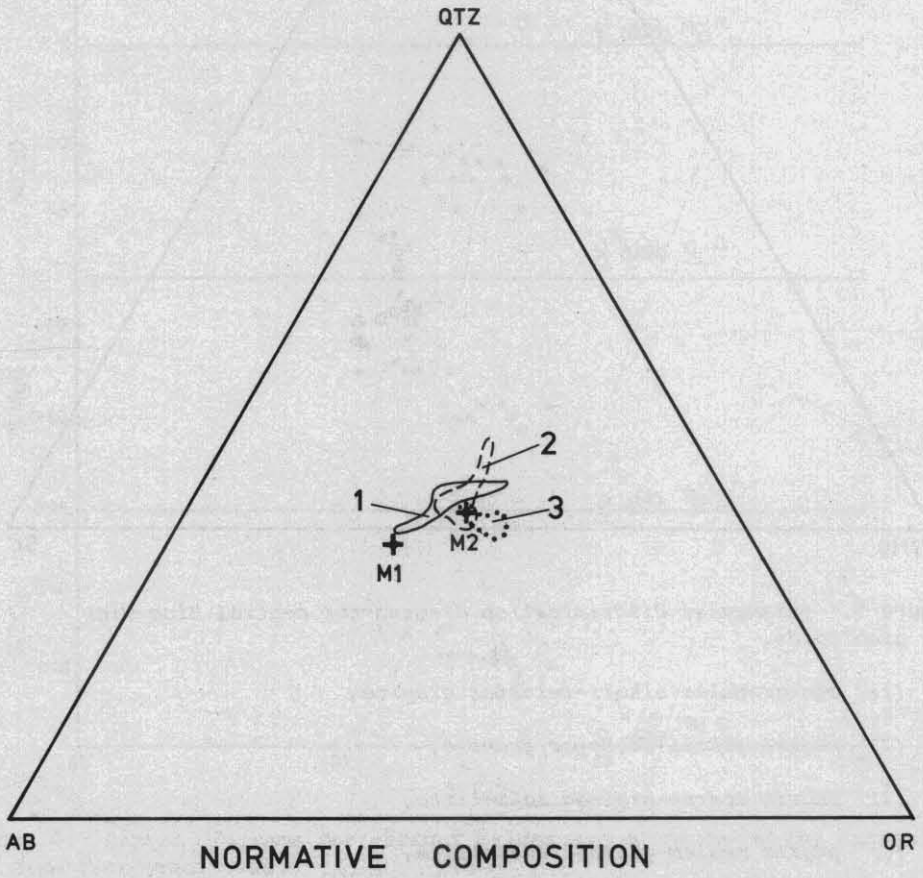

Figure 7. *Triangular plot of normative Qz-Ab-Or showing fields enclosing: (1) alkali-feldspar granite; (2) phyric coarse-grained adamellite; (3) fine and medium-grained adamellite. M1 and M2 are projections of the minimum points for 200 MPa and 50 MPa in the Qz-Ab-Or-H_2O system.*

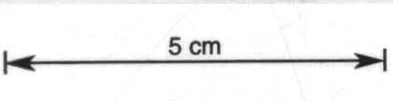

closest to the extrapolation of the adamellite trends and therefore is most likely to lie on the immediate line of evolution if a fractional crystallisation process has operated. Further fractionation to derive equigranular alkali-feldspar granite would involve a decrease in SiO_2 and K_2O and an increase in Na_2O and Al_2O_3. This may have been due to fractionation of quartz, K-feldspar, and albite from a liquid having the composition of the porphyritic alkali-feldspar granite and lying at the minimum point for the Qz-Ab-Or-H_2O system. Fractionation of these minerals would cause a build up of fluorine in the residual liquid, tending to shift the minimum composition towards the albite apex (Manning, 1981). The alkali-feldspar granite shows a trend towards the albite apex (fig. 7) with the equigranular granite, which is generally richer in fluorine than the porphyritic alkali-feldspar granite (average 4700 ppm against 2900 ppm) lying farthest in that direction, thus supporting this suggestion. The lack of exact relationship between position on the trend and fluorine content may be due to variable late stage loss of volatiles. Because the bulk major element composition of the fractionating minerals differed only slightly from that of the residual liquid, considerable fractionation may have taken place producing the large increase of Rb, Li, Nb, and P_2O_5 in the residual liquid. This model is supported by the occurrence of K-feldspar and quartz phenocrysts in the porphyritic alkali-feldspar granite, together with the textural evidence that albite was also an early crystallising phase. Minor fractionation of annite would also be expected to have occurred.

The data presented in this paper does not appear to support or refute the cumulate fractional crystallisation model of McCarthy and Groves (1979) but does indicate that the restite model alone does not provide an adequate explanation. Further progress in understanding the petrogenesis of these rocks may depend on data on rare earth elements and stable isotopes.

PRESSURE AND TEMPERATURE OF CRYSTALLISATION

The temperature of feldspar crystallisation can be obtained using the feldspar geothermometer discussed by Stormer (1975) and Whitney and Stormer (1977). This method relies upon determination of the structural state of the K-feldspar. Measurements of the lattice spacing of critical crystal planes from X-ray diffractometer charts shows that K-feldspar from adamellite has a low triclinicity (Groves *et al.*, 1977), close to orthoclase, whereas K-feldspar from alkali-feldspar granite is intermediate between orthoclase and microcline (MacKenzie, 1954; Wright and Stewart, 1968). Consequently, temperatures determined using thermodynamic parameters for microcline (Whitney and Stormer, 1977) will indicate the maximum crystallisation temperature. Determination of the bulk composition of perthitic K-feldspar was by microprobe analysis using a defocussed electron beam. Only compositions of adjacent feldspar crystals were measured in an attempt to obtain equilibrium temperatures. The mole fractions of albite in co-existing K-feldspar and plagioclase are shown in Table 8. The temperature calculated is a linear function of pressure. Feldspar temperature lines are shown on a pressure-temperature diagram in Figure 6. The calculated temperatures from co-existing feldspars in adamellite vary from 434°C to 692°C at 0 MPa but represent only the temperatures obtained from the margins of the plagioclase crystals. For the alkali-feldspar granite, perthitic K-feldspar as phenocrysts and in the matrix and assumed to be in equilibrium with plagioclase inclusions yields a constant temperature value (≈665°C at 0 MPa). The temperature calculated from the late stage, non-perthitic K-feldspar in this granite is very much lower (350°C at 0 MPa).

Table 8. FELDSPAR COMPOSITIONS (AS MOLE % Ab) AND CALCULATED TEMPERATURES, USING THE EXPRESSIONS FOR MICROCLINE (WHITNEY AND STORMER, 1977).

Rock No.	X_{Ab}^{AF}	X_{Ab}^{PF}	T°C at 0 MPa	T°C at 700 MPa
Adamellite				
735706	0.0829	0.8139	434	503
735703	0.1487	0.9053	499	574
742527	0.3333	0.8919	692	789
Alkali-feldspar granite				
742524*	0.2557	0.9681	584	668
742518*	0.2419	0.9451	579	664
802640*	0.2565	0.9829	579	664
802640†	0.0425	0.9022	350	410

* with perthitic K-feldspar
† with non-perthitic K-feldspar

A plot of the adamellite and alkali-feldspar granite on the water saturated Qz-Ab-Or system (fig. 7) shows that they both lie close to the 50 MPa minimum and therefore can be expected to have crystallised at about that pressure. The use of the data for the water saturated system is justified for the alkali-feldspar granite at least, as it contains miarolytic cavities (McCarthy and Groves, 1979). Examination of the pressure-temperature diagram (fig. 6) shows that probably all of the feldspar temperatures obtained from the adamellite were due to sub-solidus re-equilibration, as they lie on the low-temperature side of the solidus line at 50 MPa. These temperatures were only obtained from the margins of plagioclase crystals and do not prove that the remainder of the plagioclase which, due to zoning, is more anorthite rich, did not crystallise at a higher temperature in equilibrium with K-feldspar of a different composition. The temperature calculated from co-existing feldspars in the alkali-feldspar granite also appears to represent a sub-solidus temperature at 50 MPa. However the textural evidence for the perthitic K-feldspar phenocrysts used to obtain the temperature indicates that they crystallised from the magma. The high fluorine content of the alkali-feldspar granite may resolve this contradiction, because the presence of fluorine in a granitic melt substantially lowers the temperature of the solidus (Manning, 1981). Boron and lithium also reduce the solidus temperature (Chorlton and Martin, 1978; Wyllie and Tuttle, 1964). The alkali-feldspar granites are rich in Li and probably also in B, because tourmaline is present as an accessory mineral and as nodules up to 100 mm in diameter, and so these elements may add to the effect of F in lowering the solidus temperature (Manning, 1981). A considerable depression of the solidus temperature would be required to allow crystallisation of feldspar of the measured composition at a pressure close to 50 MPa, but this seems the most probable explanation. The temperature calculated from the late stage non-perthitic K-feldspar (350°C at 0 MPa) is even lower and must represent sub-solidus re-equilibration which is in agreement with the textural evidence.

CONCLUSIONS

Detailed field work in the central Blue Tier area has allowed the subdivision of granitoids to be placed on a petrologically significant basis. Alkali-feldspar granite contains albite as the only volumetrically significant plagioclase whereas adamellite contains oligoclase-andesine greatly in

excess of albite, which occurs only as narrow rims around more calcic plagioclase. Adamellite bodies which are physically similar to alkali-feldspar granite require petrographic examination to enable the distinction to be made. The alkali-feldspar granite at Blue Tier intrudes adamellite as a broad, domal body of unknown thickness. It cannot reasonably be inferred to be a sheet (Gee and Groves, 1971; Groves and Taylor, 1973). The adamellite bodies are complex, ranging in form from large plutons to small domes and thin sheets.

Although the textures of the granitoids suggest that they are magmatic, it is difficult to establish a consistent hierarchy of crystallisation in each body. It is inferred that crystallisation of the bulk of most minerals was contemporaneous, although small plagioclase and biotite crystals in K-feldspar phenocrysts suggests that these phases at least commenced crystallisation early. The textural relationships of large, clear muscovite flakes is equivocal, but abundant secondary muscovite is present. Late stage, sub-solidus alteration of all granitoids is widespread, with iron oxides, ilmenite, chlorite, muscovite, hydromica(?), epidote, and sphene being produced largely by the breakdown of biotite and feldspar. The presence of albite rims and albite veinlets suggests that sub-solidus feldspar re-equilibration occurred. The assemblages of breakdown products are different in adamellite and alkali-feldspar granite bodies, and in particular no chlorite has been discovered in alkali-feldspar granite, except in association with rare garnet. The primary mica compositions also distinguish the major granitoids. This distinctive secondary mineral assemblage provides a petrographic means of determining the original affinities of strongly altered types, and hence it is concluded that the greisenised granite south-east of Lottah is derived from adamellite.

The two major granitoid groups are also distinct in their whole rock geochemistry (see Figures 4, 5). The straight-line trends of chemical compositions on Harker variation diagrams could be explained by either restite unmixing or fractional crystallisation for adamellite, but the difference in trends between the alkali-feldspar granite and adamellite, and the impossibility of projecting alkali-feldspar granite trend lines to reasonable source rock compositions, suggests that the alkali-feldspar granite trends are not due to unmixing and are not connected to the adamellite by a restite model alone. The alkali-feldspar granite may have been derived from the adamellite by crystal fractionation or by a combination of restite unmixing and crystal fractionation. The analysis of co-existing feldspar compositions and normative compositions suggests that the granitoids crystallised at low pressure (approximately 50 MPa), and at low temperature (approximately 660°C), and it is suggested that this low temperature may be the result of the depression of the solidus temperature due to the high activity of fluorine, boron, and lithium.

ACKNOWLEDGEMENTS

We thank E. Williams for encouraging and supervising the field work at Blue Tier and E. Williams, N.J. Turner, P. Baillie, A.J.R. White, B.W. Chappell, D.R. Wones and R. Varne for discussions in the field. We acknowledge the use of the electron microscope at the University of Tasmania Central Science Laboratory.

REFERENCES

BAILLIE, P.W.; TURNER, N.J.; COX, S.F. 1978. Geological atlas 1:50 000 series. Zone 7 Sheet 24 [8416S]. Boobyalla. *Department of Mines, Tasmania*.

BROWN, A.V.; McCLENAGHAN, M.P.; MOORE, W.R.; TURNER, N.J.; McCLENAGHAN, J.; WILLIAMS, P.R.; BAILLIE, P.W.; CORBETT, K.D.; CORBETT, E.B.; COX S.F.; GROVES, D.I.; PIKE, G.P. 1977. Geological atlas 1:50 000 series. Zone 7 Sheet 32 [8415N]. Ringarooma. *Department of Mines, Tasmania*.

CHORLTON, L.B.; MARTIN, R.F. 1978. The effect of boron on the granite solidus. *Can.Mineral.* 16:239-244.

COCKER, J.D. 1977. The geology of the St Helens area. *Bull.geol.Surv. Tasm.* 55.

GEE, R.D.; GROVES, D.I. 1971. Structural features and mode of emplacement of part of the Blue Tier Batholith in north east Tasmania. *J.geol.Soc. Aust.* 18:41-55.

GRIFFIN, B.J. 1979. Energy dispersive analysis system calibration and operation with TAS-SUEDS, an advanced interactive data reduction package. *Publ.Dep.geol.Univ.Tasm.*

GROVES, D.I. 1972. The geochemical evolution of tin-bearing granites in the Blue Tier Batholith, Tasmania. *Econ.Geol.* 67:445-457.

GROVES, D.I.; COCKER, J.D.; JENNINGS, D.J. 1977. The Blue Tier Batholith. *Bull.geol.Surv.Tasm.* 55.

GROVES, D.I.; McCARTHY, T.S. 1978. Fractional crystallization and the origin of tin deposits in granitoids. *Miner.Deposita.* 13:11-26.

GROVES, D.I.; TAYLOR, R.G. 1973. Greisenization and mineralization at Anchor tin mine, north east Tasmania. *Trans.Instn.Min.Metall.* 82B:135-146.

LEAMAN, D.E.; SYMONDS, P.A. 1975. Gravity survey of north-eastern Tasmania. *Pap.geol.Surv.Tasm.* 2.

Le MAITRE, R.W. 1979. A new generalised petrological mixing model. *Contrib.Mineral.Petrol.* 71:133-137.

LUTH, W.C.; JAHNS, R.H.; TUTTLE, O.F. 1964. The granite system at pressures of 4 to 10 kilobars. *J.geophys.Res.* 69:759-773.

MANNING, D.A.C. 1981. The effect of fluorine on liquidus phase relationships in the system Qz-Ab-Or with excess water at 1 Kb. *Contrib. Mineral.Petrol.* 76:206-215.

McCARTHY, T.S.; GROVES, D.I. 1979. The Blue Tier Batholith, northeastern Tasmania. A cumulate-like product of fractional crystallisation. *Contrib.Mineral.Petrol.* 71:193-209.

McCLENAGHAN, M.P.; TURNER, N.J.; BAILLIE, P.W.; BROWN, A.V.; WILLIAMS, P.R.; MOORE, W.R. 1982. Geology of the Ringarooma-Boobyalla area. *Bull.geol.Surv.Tasm.* 61.

McCLENAGHAN, M.P.; WILLIAMS, P.R. 1981. Distribution of major granitoid bodies in the Blue Tier Quadrangle. *Unpubl.Rep.Dep.Mines Tasm.* 1981/22.

McCLENAGHAN, M.P.; WILLIAMS, P.R. In prep. Geological atlas 1:50 000 series. Zone 7 Sheet 33 [8515N]. Blue Tier. *Department of Mines, Tasmania.*

McDOUGALL, I.; LEGGO, P.J. 1965. Isotopic age determinations on granitic rocks from Tasmania. *J.geol.Soc.Aust.* 12:295-332.

MacKENZIE, W.S. 1954. The orthoclase-microcline inversion. *Mineral.Mag.* 30:354-366.

ORVILLE, P.M. 1963. Alkali ion exchange between vapor and feldspar phases. *Am.J.Sci.* 261:201-237.

REID, A.M.; HENDERSON, Q.J. 1928. Blue Tier tin field. *Bull.geol.Surv. Tasm.* 38.

STORMER, J.C. 1975. A practical two-feldspar geothermometer. *Am.Miner* 60:667-674.

STRECKEISEN, A.L. 1973. Plutonic rocks. Classification and nomenclature recommended by the IUGS Subcommission on the Systematics of Igneous Rocks. *Geotimes.* 18(10):26-30.

TAYLOR, S.R. 1965. The application of trace element data to problems in petrology. *Phys.Chem.Earth.* 6:133-213.

THOMAS, D.E. 1943. Tin deposits of the Blue Tier district. *Unpubl.Rep. Dep.Mines Tasm.* 1943:35-73.

WHITE, A.J.R.; CHAPPELL, B.W. 1977. Ultrametamorphism and granitoid genesis. *Tectonophysics.* 43:7-22.

WHITNEY, J.A.; STORMER, J.C. 1977. The distribution of $NaAlSi_3O_8$ between co-existing microcline and plagioclase and its effect on geothermometric calculations. *Am.Miner.* 62:687-691.

WRIGHT, T.L.; STEWART, D.B. 1968. X-ray and optical study of alkali feldspar. I. Determination of composition and structural state from refined unit-cell parameters and 2V. *Am.Miner.* 53:38-87.

WYLLIE, P.J.; TUTTLE, O.F. 1964. Experimental investigation of silicate systems containing two volatile components. Part III. The effects of SO_3, P_2O_5, HCl and Li_2O in addition to H_2O, on the melting temperatures of albite and granite. *Am.J.Sci.* 262:930-939.

YODER, H.S.; STEWART, D.B.; SMITH, J.R. 1957. Ternary feldspars. *Yearbook Carnegie Inst.* 56:206-214.

APPENDIX 1

Analytical conditions

The microprobe analyses were obtained at the University of Tasmania Central Science Laboratory using a JEOL JXA-50A electron microprobe analyser. The accelerating voltage was 15kV and the absorbed current was 2.1×10^{-9}A calibrated on a pure Cu standard. The position of Cu-Lα and Cu-Kα were examined and the ratio L/K was calculated. The mineral standard clinopyroxene from Delegate, N.S.W. was additionally analysed to confirm the calibration on the pure Cu standard. Data reduction was carried out interactively using program TAS-SUEDS (Griffin, 1979).